

Electronic Supplementary Information

Nematic Liquid Crystal Induces and Amplifies Circularly Polarized Luminescence of Chiral TADF Emitter

Yingyu Zhu,^a Zhanxiang Chen,^a Ao Ying,^a Shaolong Gong,^a Tao Wang,^b Chuluo Yang^{*ab}

^aDepartment of Chemistry, Renmin Hospital of Wuhan University, Hubei Key Lab on Organic and Polymeric Optoelectronic Materials, Wuhan University, Wuhan 430072, P. R. China.

^bShenzhen Key Laboratory of Polymer Science and Technology, College of Materials Science and Engineering, Shenzhen University, Shenzhen 518060, P. R. China.

*Corresponding Author E-mail Address: clyang@whu.edu.cn

Table of Contents

1. General Information

2. Theoretical Calculation

3. Photophysical Characterization

4. Synthetic and Characterization

5. Supplementary Figures

6. Reference

1. General Information

All the reagents were received from commercial sources and used without further purification. ^1H NMR and ^{13}C NMR spectra were measured by Bruker Advanced II (400 MHz) spectrometers or MERCURYVX300. Differential scanning calorimetry (DSC) was performed on a NETZSCH DSC 200 PC and Thermogravimetric analysis (TGA) was undertaken with a NETZSCH STA 449C instrument. Cyclic voltammetry (CV) was carried out in nitrogen-purged trichloromethane or *N,N*-Dimethylformamide at room temperature with a CHI voltammetric analyzer. Tetrabutylammonium hexafluorophosphate (TBAPF_6) (0.1 M) is used as the supporting electrolyte. The conventional three-electrode configuration consists of a platinum working electrode, a platinum wire auxiliary electrode, and an Ag wire pseudo-reference electrode with ferrocenium-ferrocene (Fc^+/Fc) as the internal standard.

2. Theoretical Calculation

Ground state structures and FMOs were obtained by B3LYP density functional method with basis set def2-SVP. The dispersion correction was conducted by Grimme's D3 version with BJ damping function.^{1,2} Time-dependent DFT with PBE0 functional and basis set def2-SVP were performed to further analysis of the excited states with the optimized ground state structures. All the above calculations were carried out with the Gaussian16 program.

3. Photophysical Characterization

Absorption spectra were characterized by a UV-vis-NIR spectrophotometer (UV-1650 PC or UV-2700, Shimadzu). Photoluminescence (PL) spectra, photoluminescence quantum efficiencies (Φ_{PLS}), and phosphorescence spectra were characterized by a spectrofluorimeter (FluoroMax-P, Horiba Jobin Yvon Inc. or F-4600, Hitachi Inc.). Phosphorescence spectra of toluene were measured at 77 K (the liquid nitrogen temperature) by these spectrofluorimeters equipped with a microsecond flash lamp as the pulsed excitation source. Time-resolved PL (PL decay curves) was measured by

monitoring the decay of the intensity at the PL peak wavelength using the time-correlated single-photon counting fluorescence lifetime system FLS920 of Edinburgh Instruments using a picosecond pulsed UV-LASTER (LASTER377) as the excitation source. The samples were placed in a vacuum cryostat chamber with temperature control. CD spectra were performed by Jasco-810 spectropolarimeter (Jasco, Easton, MD, USA). CPL spectra were performed by a JASCO CPL-300 spectrometer.

The rate constants were calculated according to the reported literature⁴ with the assumption that $k_{\text{RISC}} \gg k_{\text{r,T}} + k_{\text{nr,T}}$, where k_{RISC} , $k_{\text{r,T}}$ and $k_{\text{nr,T}}$ represented the rate constants of the RISC process, the radiative decay and non-radiative decay from T_1 to S_0 states, respectively. The rate constant of radiative decay from S_1 to S_0 states ($k_{\text{r,S}}$), non-radiative decay ($k_{\text{nr,S}}$), reverse intersystem crossing (k_{RISC}) and intersystem crossing (k_{ISC}) could be obtained via equations 1-4 as follows:

$$k_{\text{r,S}} = \Phi_{\text{p}}k_{\text{p}} + \Phi_{\text{d}}k_{\text{d}} \quad (1)$$

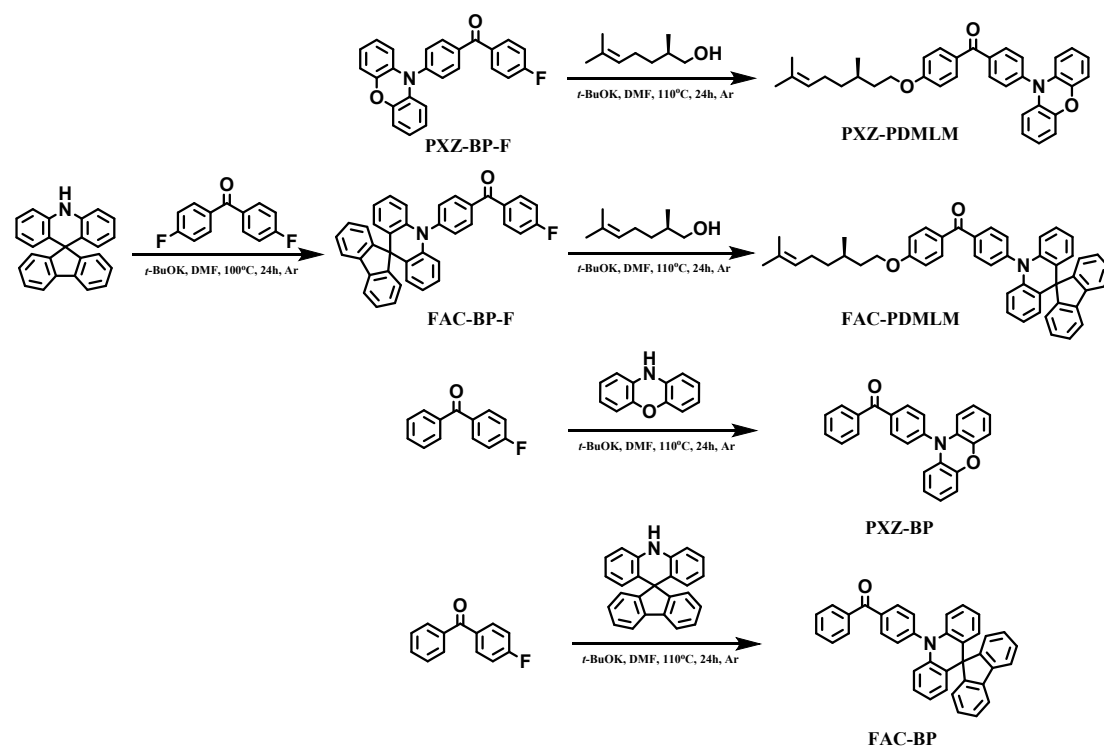
$$k_{\text{nr,S}} = (1 - \Phi_{\text{PL}})k_{\text{r,S}}/\Phi_{\text{PL}} \quad (2)$$

$$k_{\text{RISC}} \approx k_{\text{p}}k_{\text{d}}\Phi_{\text{PL}}/k_{\text{r,S}} \quad (3)$$

$$k_{\text{ISC}} \approx k_{\text{p}}k_{\text{d}}\Phi_{\text{d}}/k_{\text{RISC}}\Phi_{\text{P}} \quad (4)$$

where k_{p} and k_{d} represented the decay rate constants for prompt and delayed fluorescence, Φ_{P} and Φ_{d} represented quantum yields for the prompt and delayed fluorescence components.

4. Synthetic and Characterization



Scheme S1. The synthesis procedure of PXZ-PDMLM, FAC-PDMLM, PXZ-BP and FAC-BP.

Synthesis of ((4-(10H-phenoxazin-10-yl)phenyl)(4-fluorophenyl)methanone (PXZ-BP-F) was according to the reported literature.³

Synthesis of (4-(10H-spiro[acridine-9,9'-fluorene]-10-yl)phenyl)(4-fluorophenyl)methanone (FAC-BP-F). A mixture of 10H-spiro[acridine-9,9'-fluorene] (3.31 g, 10.0 mmol), bis(4-fluorophenyl)methanone (2.73 g, 12.5 mmol) and *t*-BuOK (1.12 g, 10.0 mmol) in 20 mL of dry DMF in a 100 mL round bottle was refluxed for 24 h under argon. After cooling down to room temperature, the reaction was quenched by cold water and then extracted with dichloromethane for three times. The combined organic extracts were dried over Na₂SO₄ and concentrated by rotary evaporation. The crude product was purified by column chromatography on silica gel to afford bright yellow powder (3.32 g, 62% yield). ¹H NMR (400 MHz, CD₂Cl₂) δ (ppm): 8.05 (m, 2H), 7.91 (m, 2H), 7.76 (m, 2H), 7.59 (m, 2H), 7.33 (m, 4H), 7.20 (m, 4H), 6.88 (m, 2H), 6.51 (m, 2H), 6.32 (m, 4H). ¹³C NMR (100 MHz, CD₂Cl₂) δ (ppm): 156.4, 144.9,

140.9, 139.3, 137.6, 132.7, 131.4, 128.4, 127.8, 127.6, 127.3, 125.5, 124.9, 120.8, 120.1, 115.7, 115.5, 114.7.

Synthesis of PXZ-PDMLM. A mixture of PXZ-BP-F (1.14 g, 2.99 mmol), (R)-2,6-dimethylhept-5-en-1-ol (0.78 g, 5.5 mmol), and *t*-BuOK (0.56 g, 5.0 mmol) in 10 mL of dry DMF in a 50 mL round bottle was refluxed for 24 h under argon. After cooling down to room temperature, the reaction was quenched by cold water and then extracted with dichloromethane for three times. The combined organic extracts were dried over Na₂SO₄ and concentrated by rotary evaporation. The crude product was purified by column chromatography on silica gel to afford bright yellow powder (0.66 g, 42% yield). ¹H NMR (400 MHz, CD₂Cl₂) δ (ppm): 7.89 (d, *J* = 8.0 Hz, 2H), 7.79 (d, *J* = 8.8 Hz, 2H), 7.40 (d, *J* = 8.4 Hz, 2H), 6.92 (d, *J* = 8.8 Hz, 2H), 6.59 (m, 6H), 5.94 (m, 2H), 5.04 (m, 1H), 4.03 (m, 2H), 1.94 (m, 1H), 1.64 (d, *J* = 5.6 Hz, 2H), 1.61 (m, 2H), 1.18 (m, 3H), 0.90 (d, *J* = 6.4 Hz, 3H), 0.80 (m, 3H). ¹³C NMR (100 MHz, CD₂Cl₂) δ (ppm): 163.2, 144.0, 142.2, 138.4, 133.9, 132.5, 132.4, 130.6, 124.6, 123.3, 121.6, 115.4, 114.1, 113.9, 113.4, 66.8, 37.1, 35.9, 29.5, 25.4, 19.3, 17.3. HRMS *m/z* calcd for C₃₅H₃₆NO₃⁺ (M + H)⁺ 518.2690, found 518.2683.

Synthesis of FAC-PDMLM. A mixture of FAC-BP-F (1.59 g, 3.00 mmol), (R)-2,6-dimethylhept-5-en-1-ol (0.78 g 5.5 mmol), and *t*-BuOK (0.56 g, 5.0 mmol) in 10 mL of dry DMF in a 50 mL round bottle was refluxed for 24 h under argon. After cooling down to room temperature, the reaction was quenched by cold water and then extracted with dichloromethane for three times. The combined organic extracts were dried over Na₂SO₄ and concentrated by rotary evaporation. The crude product was purified by column chromatography on silica gel to afford white powder (1.12 g, 56% yield). ¹H NMR (400 MHz, CD₂Cl₂) δ (ppm): 8.02 (m, 2H), 7.86 (m, 2H), 7.76 (m, 2H), 7.56 (d, *J* = 8.4 Hz, 2H), 7.34 (m, 4H), 7.21 (m, 2H), 6.96 (m, 2H), 6.88 (m, 2H), 6.51 (m, 2H), 6.33 (m, 4H), 5.05 (m, 1H), 4.05 (m, 2H), 1.95 (m, 2H), 1.81 (m, 1H), 1.61 (s, 3H), 1.54 (s, 2H), 1.19 (s, 3H), 0.91 (d, *J* = 6.4 Hz, 3H), 0.79 (m, 2H). ¹³C NMR (100 MHz, CD₂Cl₂) δ (ppm): 156.5, 141.0, 139.3, 132.5, 132.5, 131.2, 128.4, 127.7, 127.6, 127.3,

125.5, 124.9, 120.7, 120.1, 114.7, 114.2, 37.1, 36.0, 35.2, 29.5, 25.4, 19.3. HRMS m/z calcd for $C_{48}H_{44}NO_2^+$ ($M + H$)⁺ 666.3367, found 666.3358.

Synthesis of PXZ-BP. A mixture of (4-fluorophenyl)(phenyl)methanone (0.40 g, 2.0 mmol), 10*H*-phenoxazine (0.46 g, 2.5 mmol), and *t*-BuOK (0.28 g, 2.5 mmol) in 10 mL of dry DMF in a 50 mL round bottle was refluxed for 24 h under argon. After cooling down to room temperature, the reaction was quenched by cold water and then extracted with dichloromethane for three times. The combined organic extracts were dried over Na_2SO_4 and concentrated by rotary evaporation. The crude product was purified by column chromatography on silica gel to afford bright yellow powder (0.44 g, 60% yield). 1H NMR (400 MHz, $CDCl_3$) δ (ppm): 8.04 (d, $J = 8.4$ Hz, 2H), 7.87 (d, $J = 6.8$ Hz, 2H), 7.50 (m, 1H), 6.72-6.63 (m, 6H), 6.01-5.98 (m, 1H). ^{13}C NMR (100 MHz, $CDCl_3$) δ (ppm): 144.0, 143.0, 137.4, 137.1, 133.8, 132.8, 130.8, 130.0, 128.5, 123.3, 121.8, 115.7, 113.4.

Synthesis of FAC-BP. A mixture of (4-fluorophenyl)(phenyl)methanone (0.40 g, 2.0 mmol), 10*H*-spiro[acridine-9,9'-fluorene] (0.83 g, 2.5 mmol), and *t*-BuOK (0.28 g, 2.5 mmol) in 10 mL of dry DMF in a 50 mL round bottle was refluxed for 24 h under argon. After cooling down to room temperature, the reaction was quenched by cold water and then extracted with dichloromethane for three times. The combined organic extracts were dried over Na_2SO_4 and concentrated by rotary evaporation. The crude product was purified by column chromatography on silica gel to afford yellow powder (0.66 g, 65% yield). 1H NMR (400 MHz, $CDCl_3$) δ (ppm): 8.16 (d, $J = 8.4$ Hz, 2H), 7.94 (m, 2H), 7.80 (m, 2H), 7.66 (m, 3H), 7.58 (m, 2H), 7.41 (m, 4H), 7.28 (m, 2H), 6.95 (m, 2H), 6.60 (m, 2H), 6.40 (m, 4H). ^{13}C NMR (100 MHz, $CDCl_3$) δ (ppm): 156.4, 145.1, 140.8, 139.3, 132.9, 131.4, 130.1, 128.5, 128.4, 127.7, 127.3, 125.8, 121.0, 120.0.

Preparation of TADF \in 5CB systems. TADF emitter (PXZ-PDMLM or FAC-PDMLM) and 5CB were dissolved in dichloromethane. Then the mixture was heated

and stirred at 50 °C for 48 h to remove solvent.

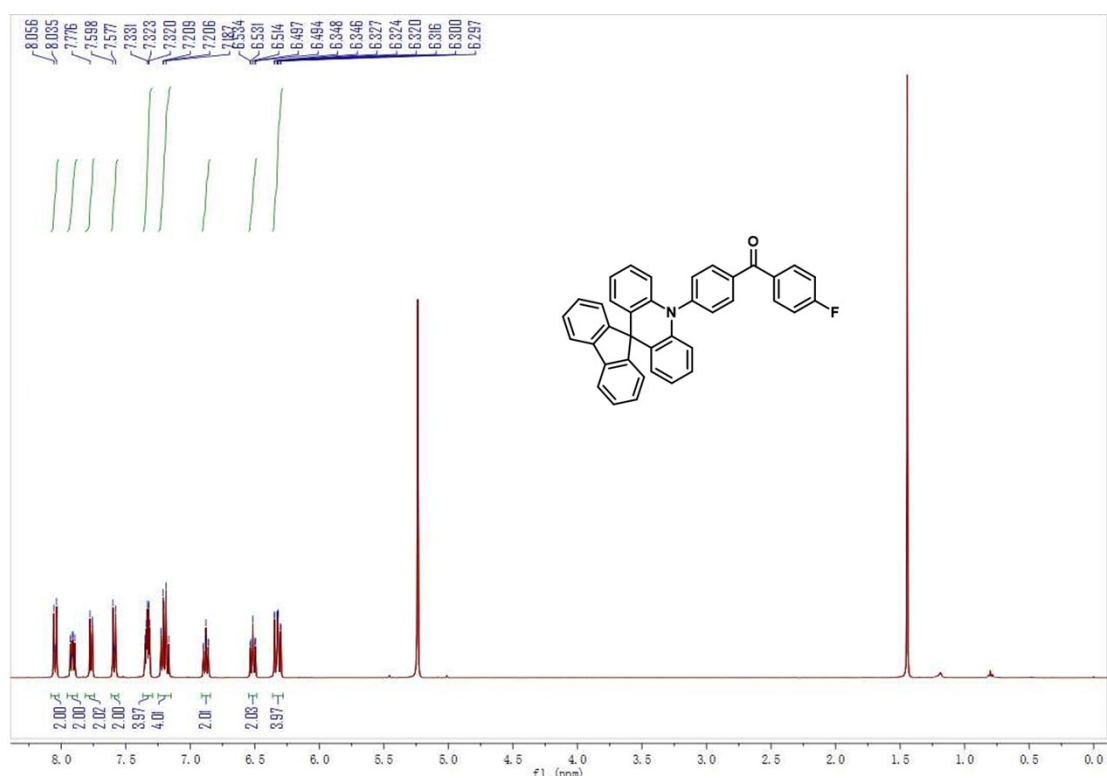


Figure S1. ¹H NMR spectrum of FAC-BP-F (400MHz, CD₂Cl₂ + TMS, 300K).

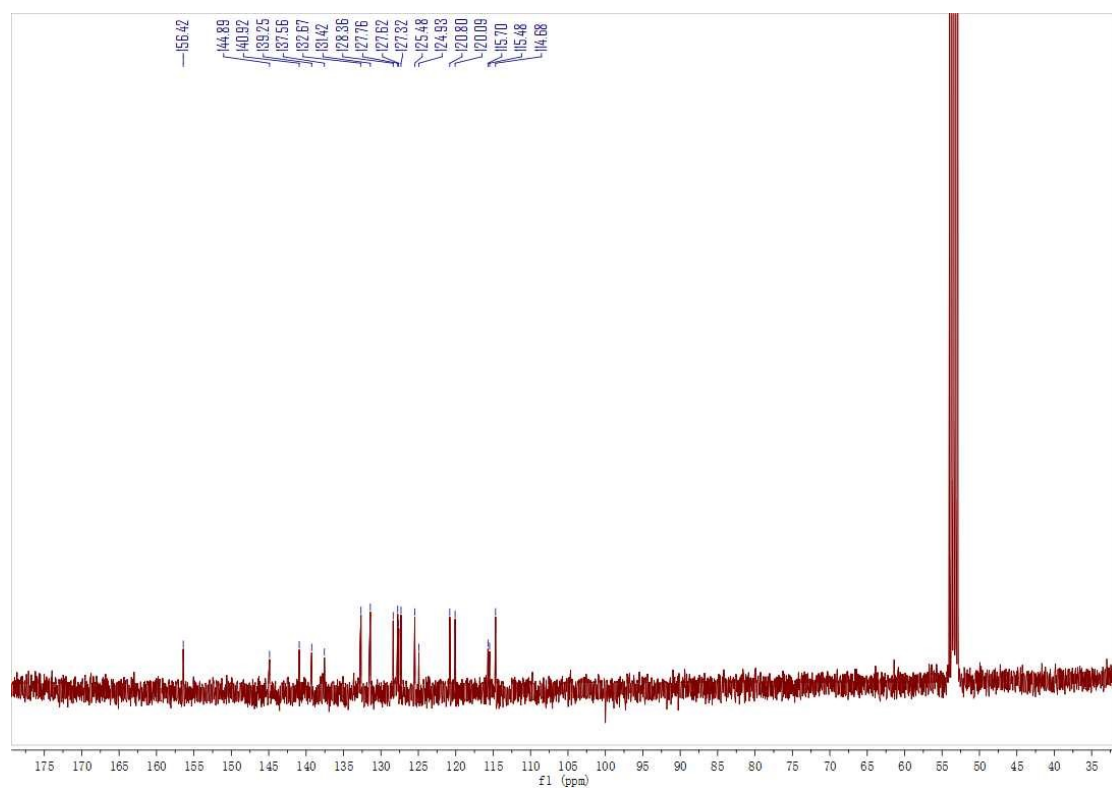


Figure S2. ¹³C NMR spectrum of FAC-BP-F (100MHz, CD₂Cl₂ + TMS, 300K).

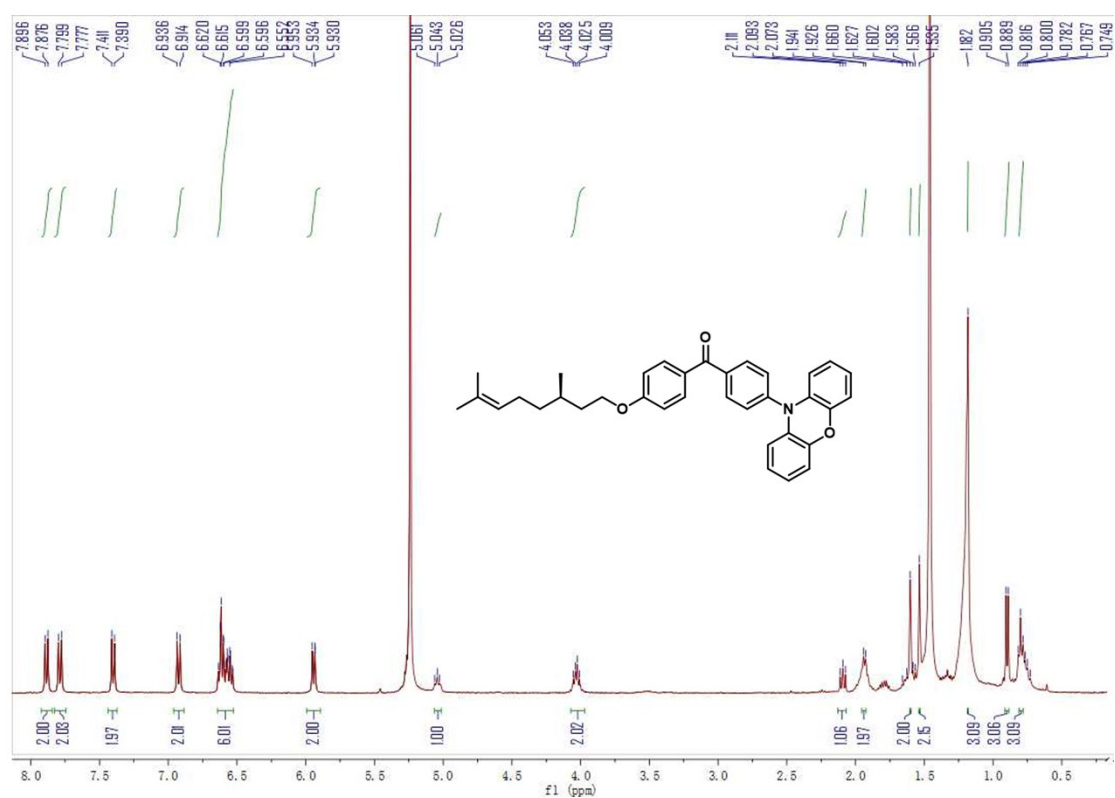


Figure S3. ^1H NMR spectrum of PXZ-PDMLM (400MHz, $\text{CD}_2\text{Cl}_2 + \text{TMS}$, 300K).

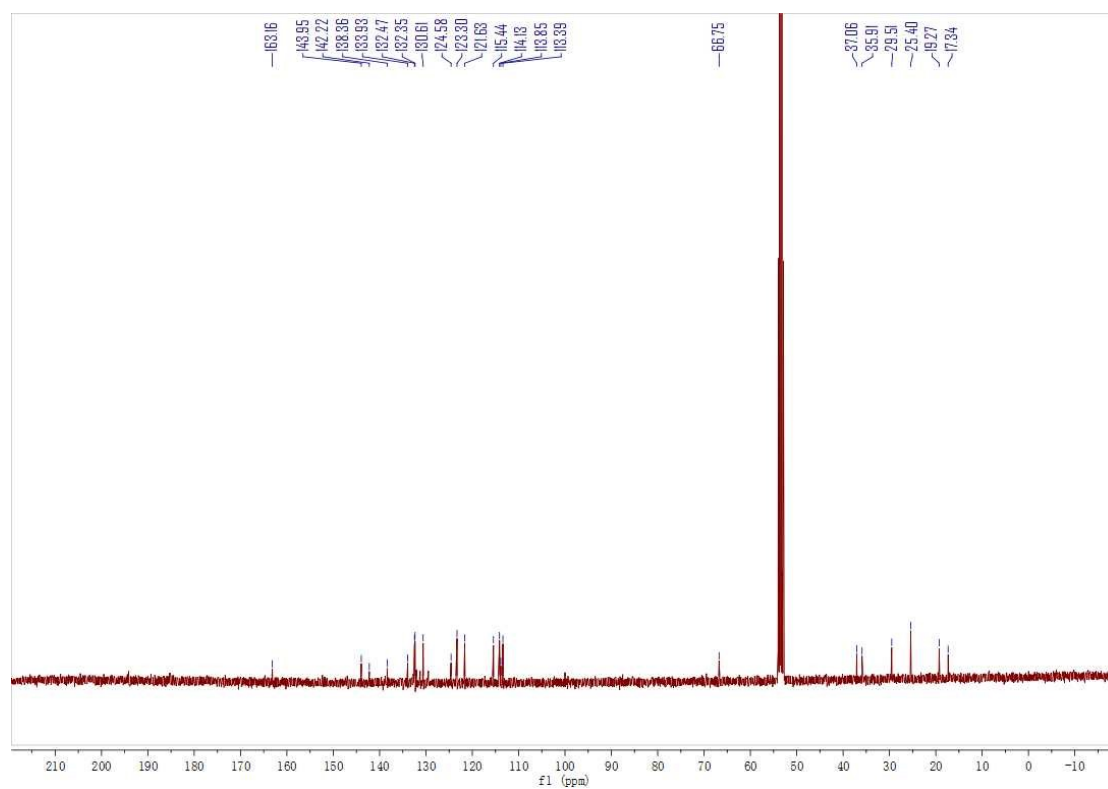
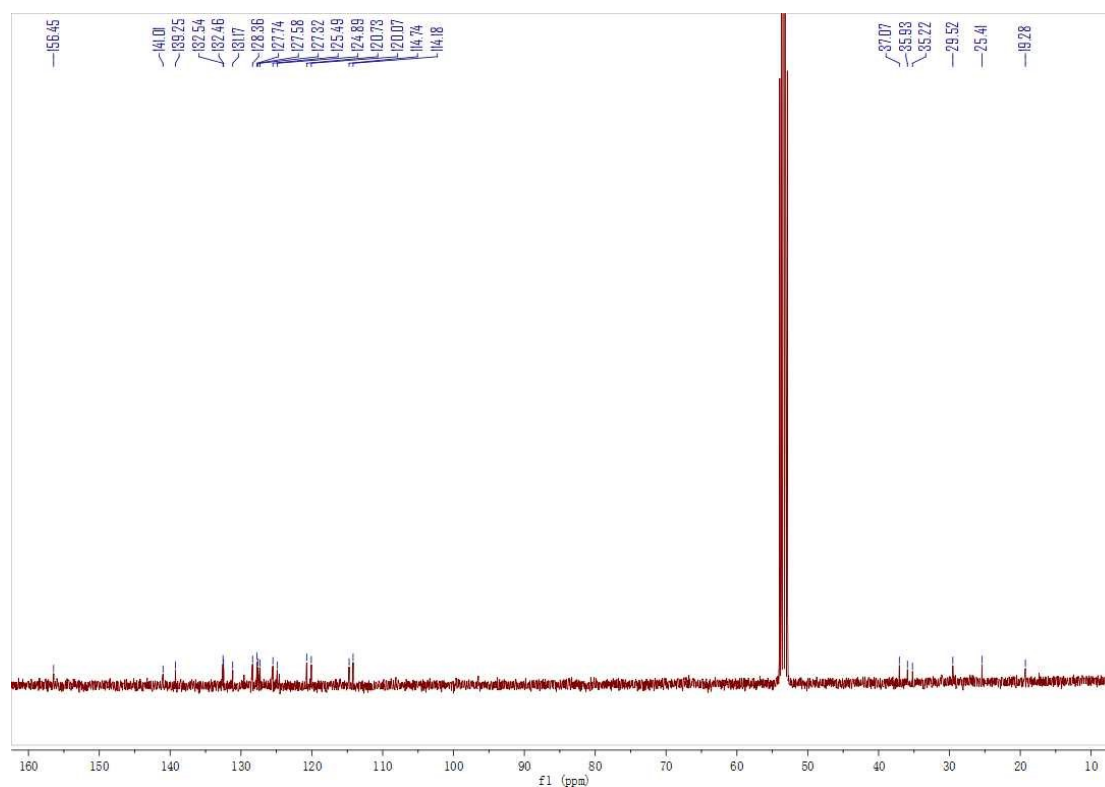
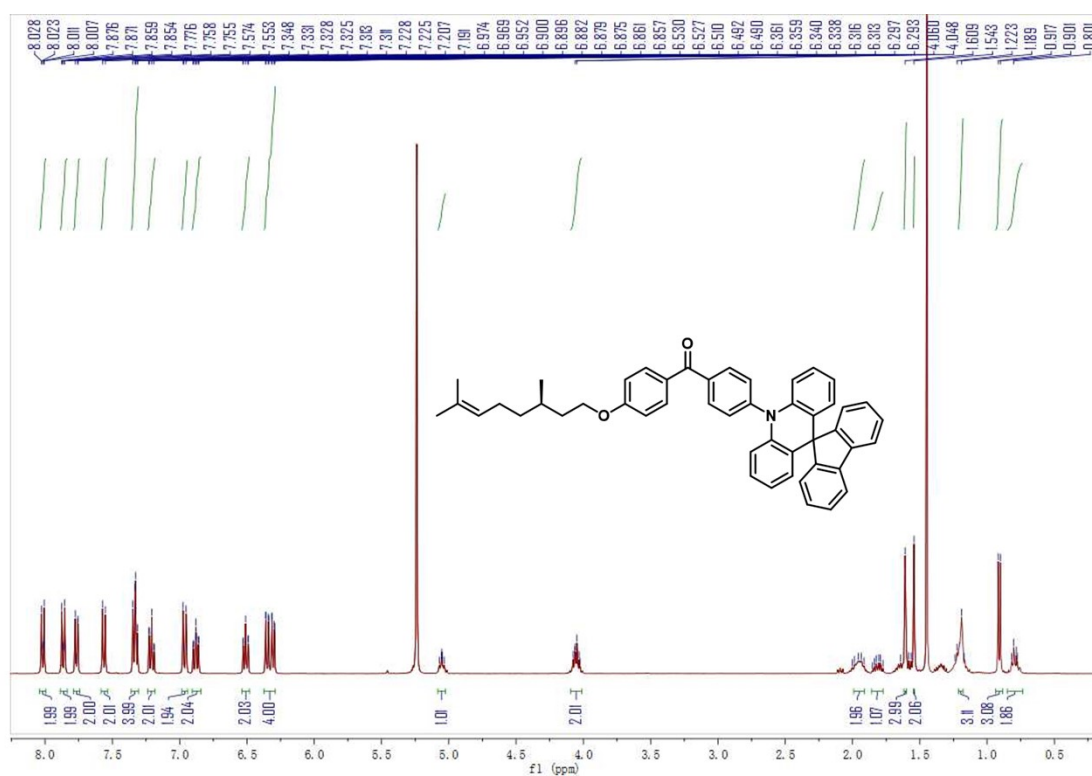


Figure S4. ^{13}C NMR spectrum of PXZ-PDMLM (100MHz, $\text{CD}_2\text{Cl}_2 + \text{TMS}$, 300K).



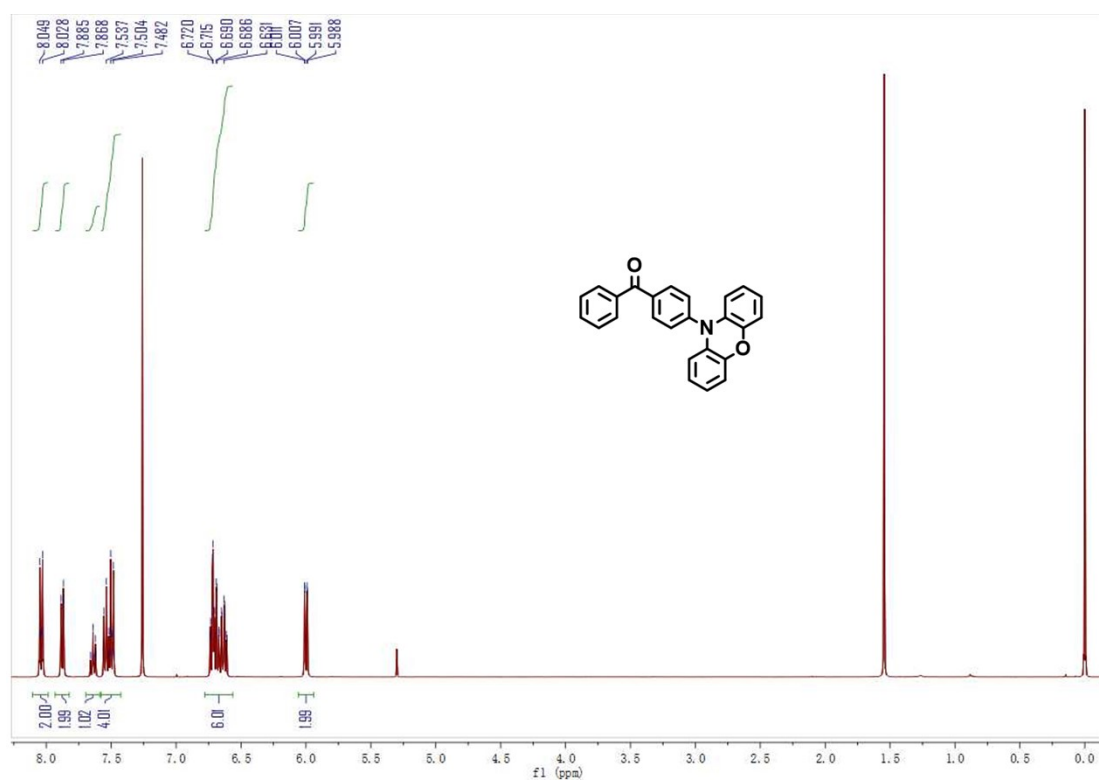


Figure S7. ^1H NMR spectrum of PXZ-BP (400MHz, CDCl_3 + TMS, 300K).

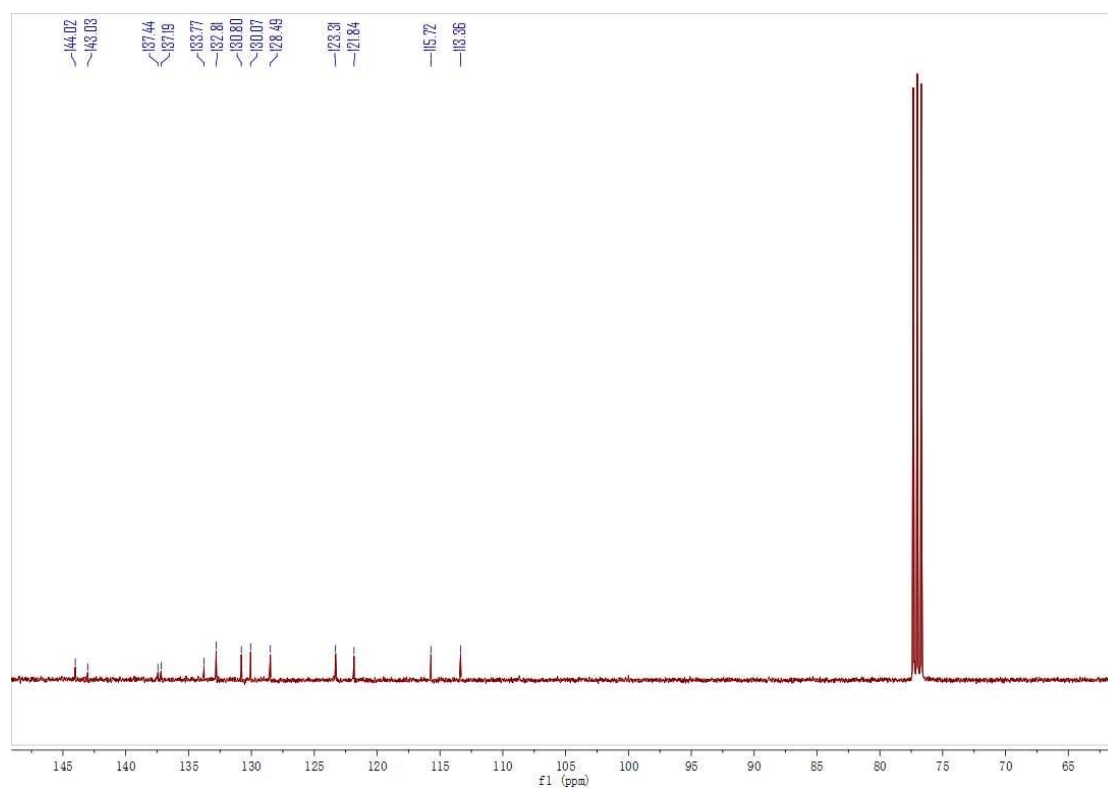


Figure S8. ^{13}C NMR spectrum of PXZ-BP (100MHz, CDCl_3 + TMS, 300K).

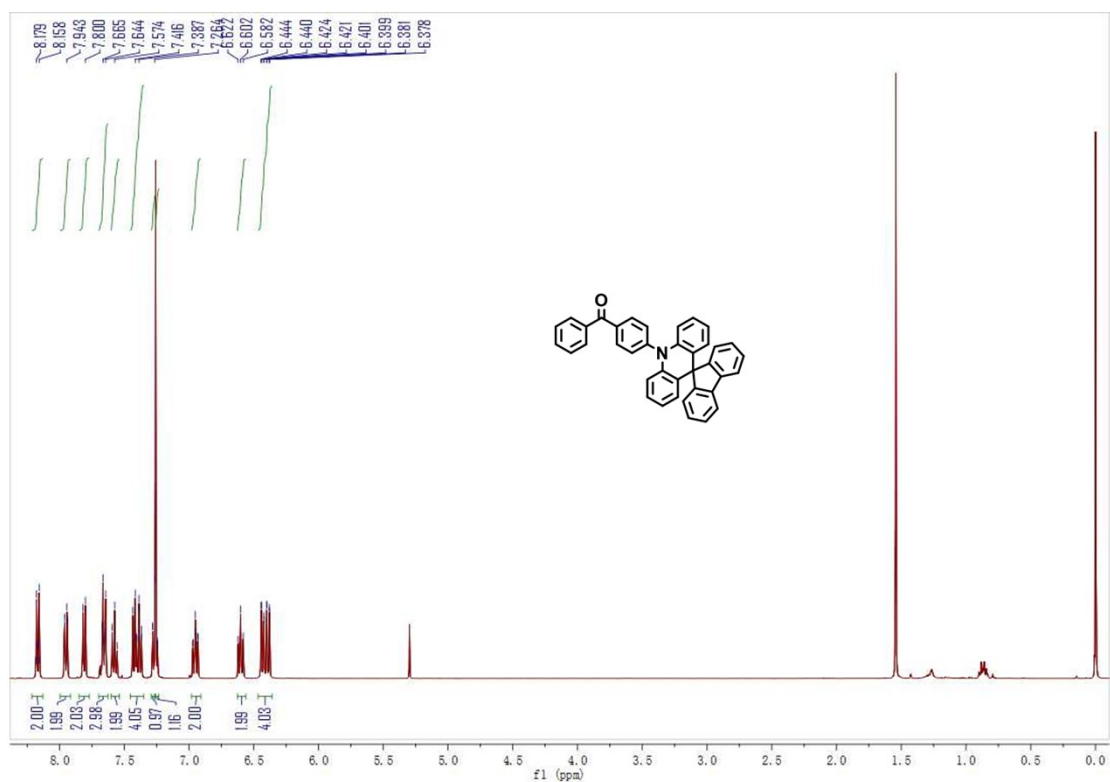


Figure S9. ^1H NMR spectrum of FAC-BP (400MHz, CDCl_3 + TMS, 300K).

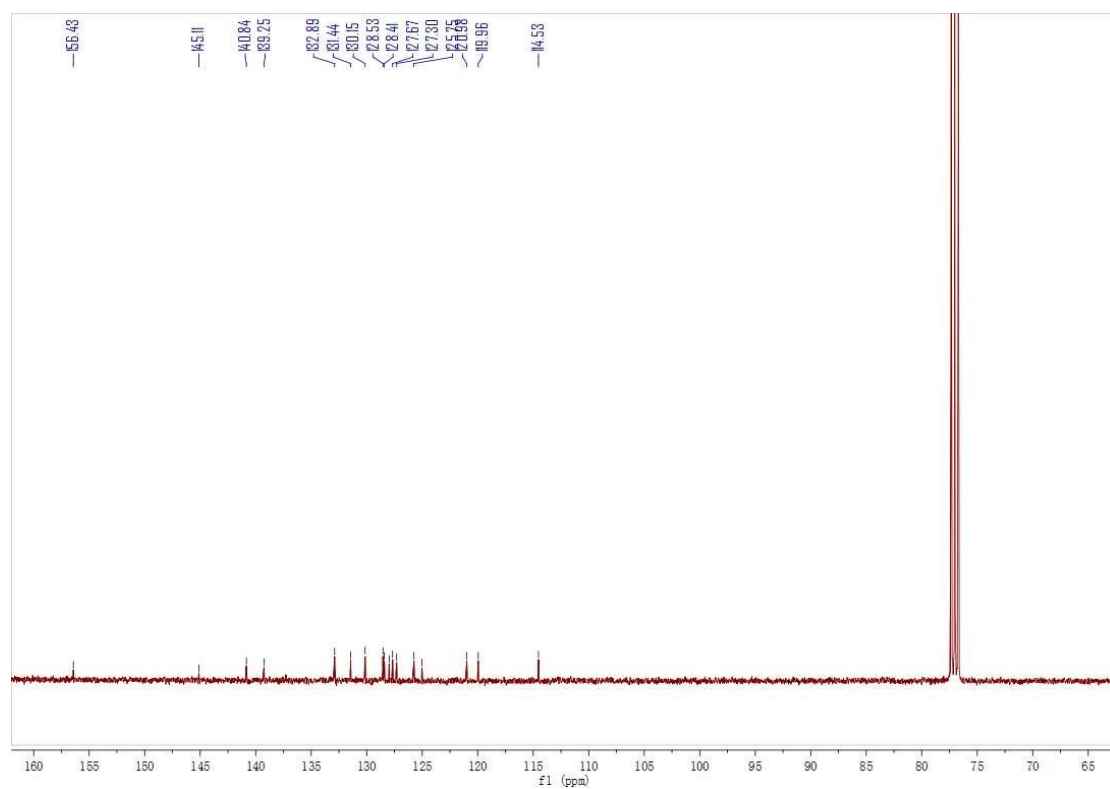


Figure S10. ^{13}C NMR spectrum of FAC-BP (100MHz, CDCl_3 + TMS, 300K).

5. Supplementary Figures

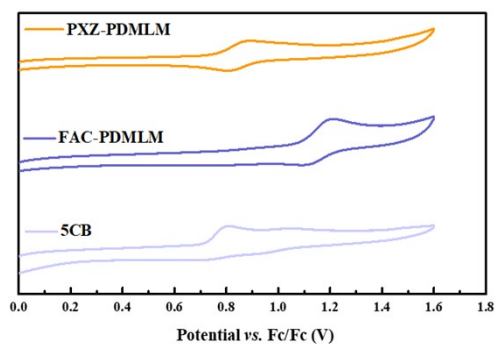


Figure S11. Cyclic voltammograms of PXZ-PDMLM, FAC-PDMLM and 5CB.

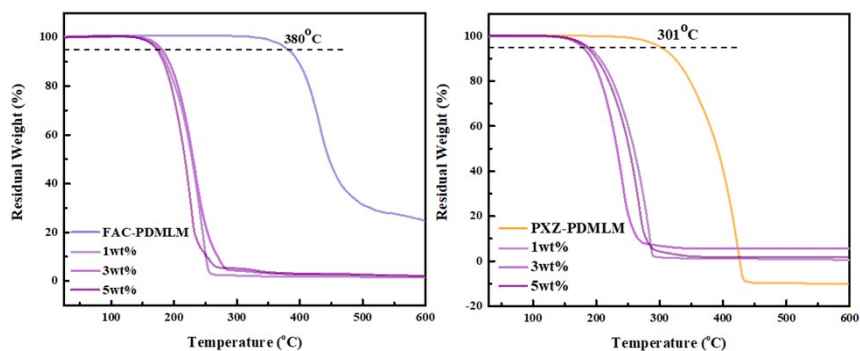


Figure S12. TGA traces of PXZ-PDMLM, FAC-PDMLM and doping in 5CB at a ratio of 1 wt%, 3 wt% and 5 wt% recorded at a heating rate of 10 °C/min.

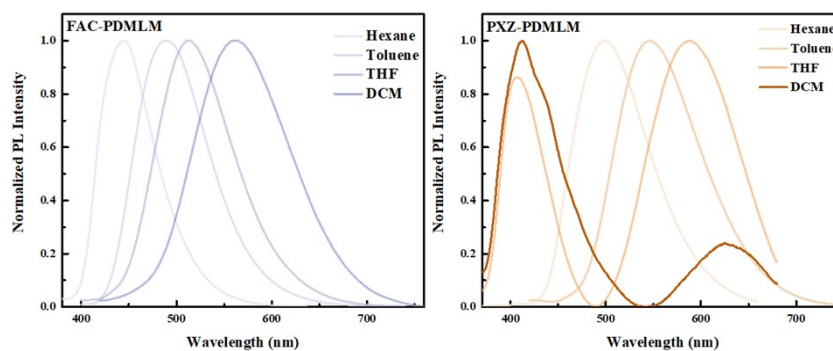


Figure S13. Normalized fluorescence spectrum in different polar solvents (10^{-5} M) of FAC-PDMLM and PXZ-PDMLM.

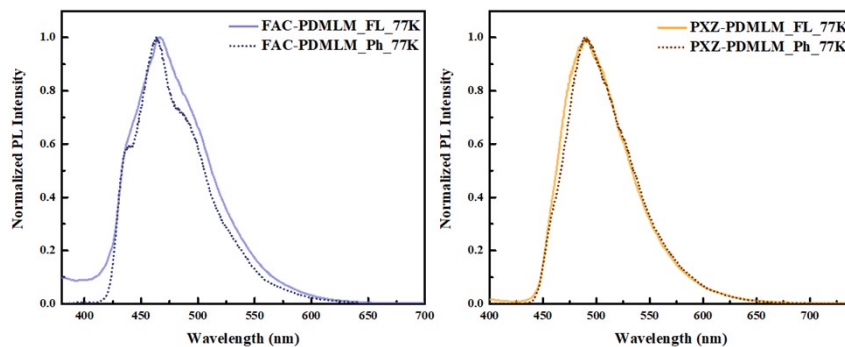


Figure S14. Normalized fluorescence and phosphorescence spectra at 77 K of FAC-PDMLM and PXZ-PDMLM.

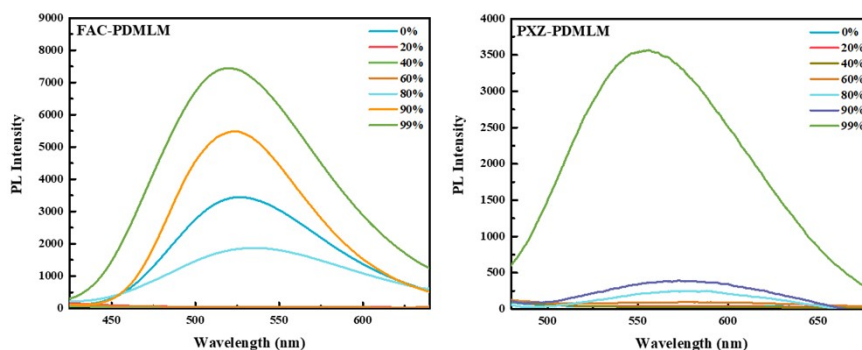


Figure S15. Fluorescence spectra of FAC-PDMLM and PXZ-PDMLM in THF/water mixtures with different water fractions ($f_w = 0\%$, 20%, 40%, 60%, 80%, 90% and 99%).

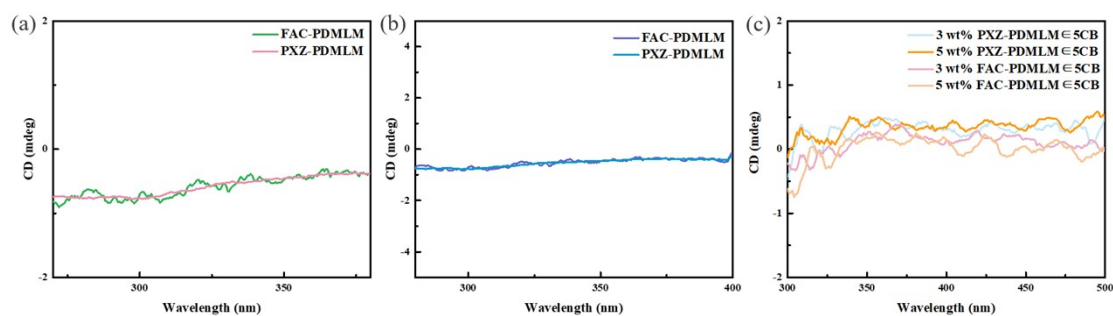


Figure S16. (a) CD spectra in 99% f_w THF/H₂O mixture of FAC-PDMLM and PXZ-PDMLM at 10 °C. (b) CD spectra in THF at 10 °C. (c) CD spectra in 3 wt%/5 wt% PXZ-PDMLM/5CB and 3 wt%/5 wt% FAC-PDMLM/5CB at 30 °C.

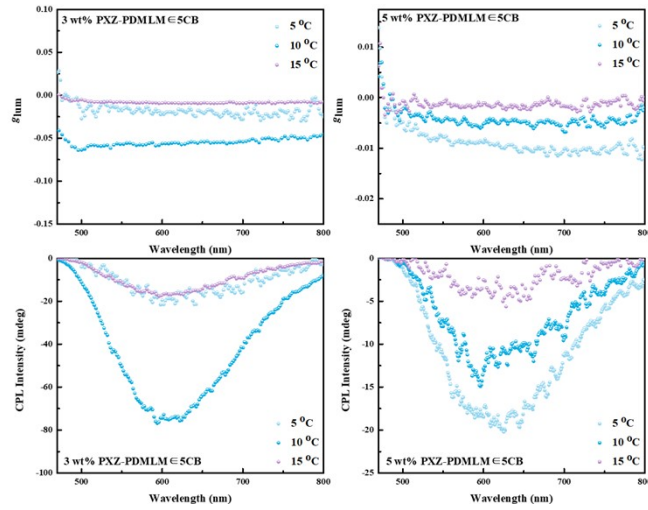


Figure S17. CPL measurement of 3 wt% and 5 wt% of PXZ-PDMLM \in 5CB from 5 to 15 °C.

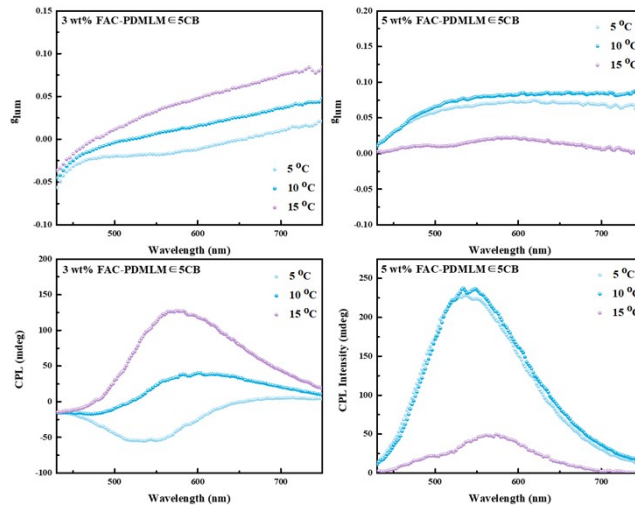


Figure S18. CPL measurement of 3 wt% and 5 wt% of FAC-PDMLM \in 5CB from 5 to 15 °C.

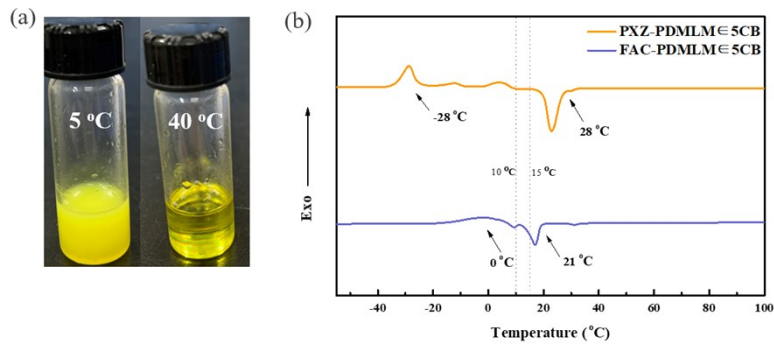


Figure S19. (a) Images of PXZ-PDMLM \in 5CB at 5 °C and 40 °C, (b) DSC traces of 3 wt% PXZ-PDMLM \in 5CB and 5 wt% FAC-PDMLM \in 5CB recorded at a heating rate of 10 °C min⁻¹.

Table S1. CPL data of FAC-PDMLM \in 5CB systems.

| Chiral TADF | Ratios (wt%) | Temperature (°C) | g_{lum} (10^{-3}) | Helical pitch (μm) |
|--------------------|---------------------|-------------------------|--|---|
| FAC-PDMLM | 3 | 5 | -9.3 | 10.4 |
| | | 10 | 12.3 | 9.9 |
| | | 15 | 39.4 | 9.6 |
| | 5 | 5 | 62.3 | 10.0 |
| | | 10 | 72.6 | 10.1 |
| | | 15 | 12.4 | 10.6 |

Table S2. CPL data of PXZ-PDMLM \in 5CB systems.

| Chiral TADF | Ratios (wt%) | Temperature (°C) | g_{lum} (10^{-3}) | Helical pitch (μm) |
|--------------------|---------------------|-------------------------|--|---|
| PXZ-PDMLM | 3 | 5 | -17.4 | 11.7 |
| | | 10 | -54.5 | 11.1 |
| | | 15 | -8.1 | 11.9 |
| | 5 | 5 | -8.6 | 4.6 |
| | | 10 | -4.1 | 5.2 |
| | | 15 | -1.2 | 5.3 |

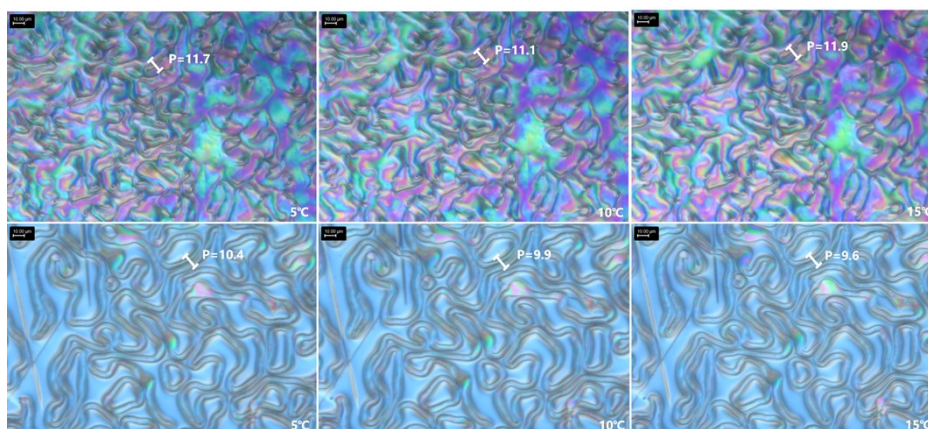


Figure S20. POM images of 3 wt% PXZ-PDMLM/5CB (above) and FAC-PDMLM/5CB (underneath) from 5 to 15 °C.

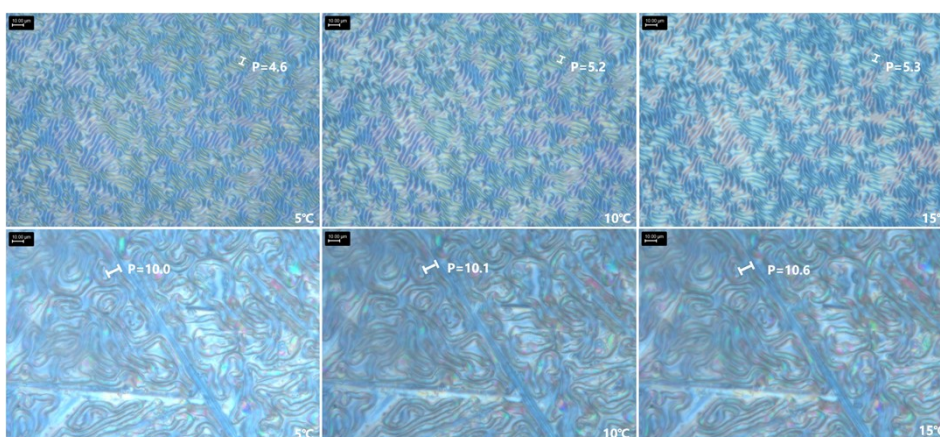


Figure S21. POM images of 5 wt% PXZ-PDMLM/5CB (above) and FAC-PDMLM/5CB (underneath) from 5 to 15 °C.

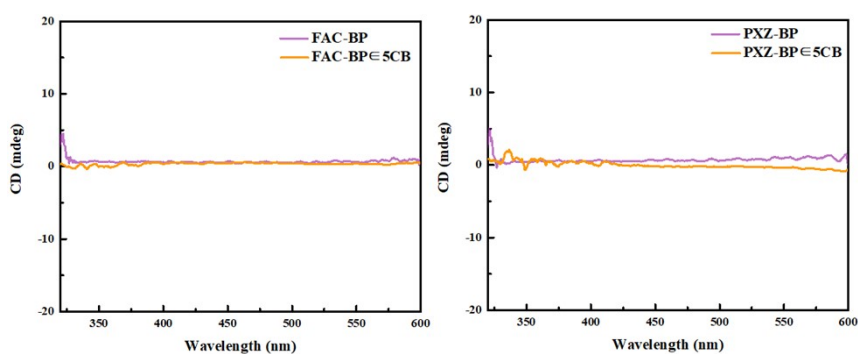


Figure S22. CD spectra in FAC-BP, FAC-BP/5CB, PXZ-BP and PXZ-BP/5CB.

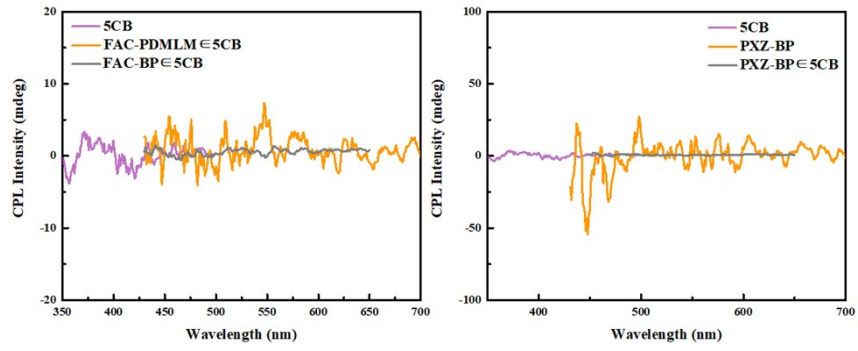


Figure S23. CPL spectra in 5CB, FAC-BP, FAC-BP ∈ 5CB, PXZ-BP and PXZ-BP ∈ 5CB.

6. Reference

- 1 S. Grimme, J. Antony, S. Ehrlich and H. Krieg, *J. Chem. Phys.*, 2010, **132**, 154104.
- 2 S. Grimme, S. Ehrlich and L. Goerigk, *J. Comput. Chem.*, 2011, **32**, 1456-1465.
- 3 J. Yang, J. Qin, P. Geng, J. Wang, M. Fang and Z. Li, *Angew. Chem., Int. Ed.*, 2018, **57**, 14174-14178.
- 4 K. -C. Pan, S. -W. Li, Y. -Y. Ho, Y. -J. Shiu, W. -L. Tsai, M. Jiao, W. -K. Lee, C. -C. Wu, C. -L. Chung, T. Chatterjee, Y. -S. Li, K. -T. Wong, H. -C. Hu, C. -C. Chen and M. -Ting. Lee, *Adv. Funct. Mater.*, 2016, **26**, 7560.